CDF/PUB/TOP/PUBLIC/7804

# Measurement of the Helicity of $W$ Bosons in Top-Quark Decays

The CDF Collaboration
August 29, 2005

**Measurement of the Helicity of $W$ Bosons in Top-Quark Decays**

The CDF Collaboration
*URL http://www-cdf.fnal.gov*
(Dated: August 29, 2005)

We measure the branching fraction of the top quark to longitudinally and right-handed polarized $W$ bosons, $F_0$ and $F_+$, using approximately 200 pb$^{-1}$ of $\bar{p}p$ collisions collected by the CDF experiment. We analyze two kinematic quantities: the invariant mass of the charged lepton and the bottom-quark jet in the decay $t \to Wb \to \ell\nu b$ (where $\ell = e$ or $\mu$), and the transverse momentum of the charged lepton. We find $F_0 = 0.74^{+0.22}_{-0.34}$ (stat. + syst.), and $F_+ < 0.27$ at the 95% confidence level. These measurements are in agreement with the Standard Model predictions.

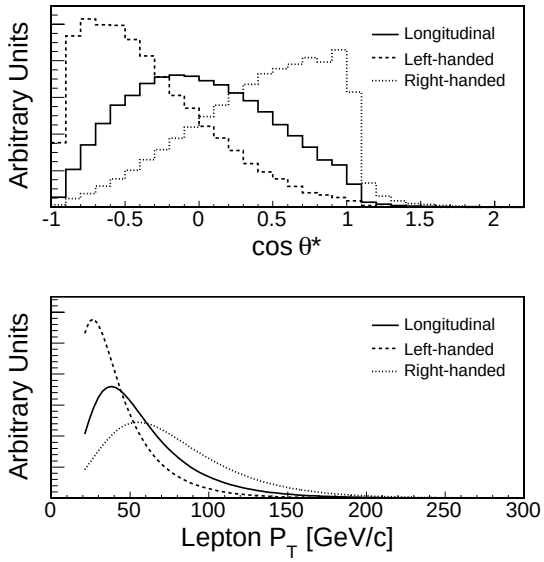


FIG. 1: Distributions of $\cos\theta^*$ (upper plot) and lepton $P_T$ (lower) for top-quark decays to left-handed, right-handed, and longitudinally polarized $W$ bosons.

The top quark is the most massive known fermion, with a mass of approximately 175 GeV/$c^2$ [1, 2]. At the Fermilab Tevatron proton-antiproton collider, with a center-of-mass energy of $\sqrt{s} = 1.96$ TeV, most top quarks are pair-produced via the strong interaction [3, 4]. However, the decay $t \to Wb$ proceeds entirely via the weak interaction. Given the $V - A$ structure of the weak interaction, in the limit of a massless bottom quark the top quark can decay to either a left-handed or longitudinally-polarized $W^+$ boson [5]. The fraction $F_0$ of longitudinally polarized $W$ bosons is enhanced due to the large coupling of the top quark to the Goldstone modes of the Higgs field. The Standard Model (SM) predicts [6]

$$F_0 \equiv \frac{\Gamma(t \to W_0 b)}{\Gamma(t \to W_0 b) + \Gamma(t \to W_\pm b)} = \frac{m_t^2}{2M_W^2 + m_t^2}, \tag{1}$$

where $W_0$ and $W_\pm$ indicate longitudinally- and transversely-polarized $W$'s respectively. For $m_t = 175$ GeV/$c^2$, $F_0 = 0.70$. A deviation from this prediction could indicate non-SM physics in top-quark decays [7], as could a nonzero value for the right-handed fraction $F_+$.

We use two observables in $t\bar{t}$ candidate events to measure the $W$ helicity. Charged leptons from the decay of a longitudinally-polarized $W$ boson have a symmetric angular distribution $\propto (1 - \cos^2\theta^*)$, where $\theta^*$ is the angle between the charged-lepton momentum in the $W$ rest frame and the boost direction from the top-quark rest frame into the $W$ rest frame. Left-handed $W$'s have an asymmetric distribution $\propto (1 - \cos\theta^*)^2$. Direct measurement of this angle is difficult, but we can approximate $\cos\theta^*$ by relating it to the invariant mass of the $b$ quark and the charged lepton:

$$\cos\theta^* = \frac{p_\ell \cdot p_b - E_\ell E_b}{|\mathbf{p}_\ell||\mathbf{p}_b|} \simeq \frac{2{M_{lb}}^2}{m_t^2 - M_W^2} - 1, \tag{2}$$

a variable that depends only on lab-frame momenta. The second observable exploits the fact that charged leptons from left-handed $W$ decays are preferentially emitted in the backward direction with respect to the $W$ direction of motion, leading to a softer lepton transverse momentum $P_T$ in the lab

frame, while the leptons from right-handed $W$'s are preferentially emitted forward and thus have a harder $P_T$ spectrum. Longitudinal $W$ decays represent an intermediate case. Figure 1 shows the predicted $\cos\theta^*$ and lepton $P_T$ distributions for $m_t = 175$ GeV/$c^2$, after the event selection and reconstruction described below.

A measurement of $F_0$ has been previously reported by the CDF Collaboration [8] using $\approx 100$ pb$^{-1}$ of data from the 1992-1996 Tevatron collider run (Run I). Using the $P_T$ technique, a value of $0.91 \pm 0.37(\text{stat}) \pm 0.13(\text{syst})$ was obtained. Using the same data set, CDF has also placed a limit on the right-handed helicity fraction of $F_+ < 0.18$ at the 95% confidence level (C.L.) with the $\cos\theta^*$ technique [9]. The DØ Collaboration has used 125 pb$^{-1}$ of Run I data to obtain $F_0 = 0.56 \pm 0.31$ using the leading-order $t\bar{t}$ matrix element to weight each event according to its decay probability for each helicity state [10]. Here, we report a measurement of $F_0$ and $F_+$ that combines the $\cos\theta^*$ and $P_T$ techniques. The data samples were collected at $\sqrt{s} = 1.96$ TeV using the CDF detector at the Fermilab Tevatron $p\bar{p}$ collider during 2000-03, and have integrated luminosities between 162 and 193 pb$^{-1}$.

The CDF II detector [11] consists of a charged-particle tracking system in a magnetic field of 1.4 T, segmented electromagnetic and hadronic calorimeters, and muon detectors. A silicon microstrip detector provides tracking over the radial range 1.5 to 28 cm, and is used to detect displaced secondary vertices. The fiducial region of the silicon detector covers the pseudo-rapidity range $|\eta| < 2$, while the central tracking system and muon chambers provide coverage for $|\eta| < 1$ [12]. A three-level trigger system selects events with electron (muon) candidates with $E_T$ ($P_T$) $> 18$ GeV (18 GeV/c), which form the data set for this analysis.

In the decay process $t\bar{t} \to W^+bW^-\bar{b}$, events can be classified based on the observed number of isolated charged leptons with large transverse momentum, where a lepton signifies an electron or muon of either charge; typically these leptons come from the decay $W \to \ell\nu$. Transverse momentum for electrons from $W$ decay is best measured at CDF using the transverse energy $E_T$ deposited in the calorimeter, while for muons the transverse momentum is best measured by the tracking system. From here on, we use the symbol $P_T$ to denote the appropriate calorimeter- or tracking-based quantity. The 193 pb$^{-1}$ "dilepton" sample [13] consists of events with two oppositely-charged, isolated leptons, each with $P_T > 20$ GeV/$c$. Events in this sample are required to have two or more jets with pseudorapidity $|\eta| < 2$ and transverse energy $E_T > 15$ GeV, and missing transverse energy $\not\!\!E_T > 25$ GeV. The scalar sum of the transverse energy of the jets, leptons, and $\not\!\!E_T$, is required to be greater than 200 GeV. We observe 13 events in this sample, with a predicted total background from $WW$ pairs, $Z \to \tau\tau$, the Drell-Yan process, and hadrons misidentified as leptons of $2.7 \pm 0.7$ events. The 162 pb$^{-1}$ "lepton plus jets" sample [14] consists of events with a single isolated lepton with $P_T > 20$ GeV, $\not\!\!E_T > 20$ GeV, and three or more jets with $|\eta| < 2$ and $E_T > 15$ GeV. To reduce QCD backgrounds, we require that one or more jets have a displaced secondary-vertex tag, indicating that it is consistent with the decay of a long-lived $b$ hadron. Fifty-seven events pass the selection cuts, of which approximately 2/3 are $t\bar{t}$ events. The largest remaining backgrounds come from QCD events, fake $b$-tags, and tags of $W$ plus jets events containing bottom or charm jets.

The $P_T$ analysis [15] uses both samples, while the $\cos\theta^*$ analysis [16] uses the lepton plus jets sample only. In addition to the selection requirements described above, events selected for the $\cos\theta^*$analysis are required to have a fourth jet with $E_T > 8$ GeV and $|\eta| < 2$. Thirty-seven events pass this cut, of which $9.9 \pm 1.7$ are estimated to be background. The presence of four jets allows the event to be kinematically reconstructed as a $t\bar{t}$ event [1] with the top mass constrained to 175 GeV/$c^2$, and to associate the appropriate jet to the lepton in Equation 2. We find that 31 of the 37 events pass a $\chi^2_{\text{min}}$ cut on the fit quality.

To create $\cos\theta^*$ (lepton $P_T$) templates for $t\bar{t}$ signal events, we use the MadEvent [17] (Herwig [18]) Monte Carlo program. We fix the helicity in the top rest frame of one $W$ boson, while the other $W$ takes on values according to the SM prediction. Hadronization and fragmentation are carried out using pythia [19], and the events are passed through the CDF simulation and reconstruction algorithms. For the lepton plus jets sample, all backgrounds except QCD are modeled with Monte Carlo simulations. We model the QCD background using lepton plus jets events where the primary lepton is non-isolated. For the dilepton sample all but the fake background is modeled with Monte Carlo. We model the fake dilepton background using lepton plus jet events containing jets that could fake a charged lepton.

TABLE I: Summary of results for the $\cos\theta^*$, $P_T$, and combined measurements of $F_0$ and $F_+$. $N$ is the number of events or leptons used in the measurement. Where two uncertainties are given the first is statistical and the second is systematic. Uncertainties on the combined measurements are the total statistical and systematic uncertainty.

| Analysis | $N$ | $F_0$ | $F_+$ |
|---|---|---|---|
| $\cos\theta^*$ | 31 | $0.99^{+0.29}_{-0.35} \pm 0.19$ | $0.23 \pm 0.16 \pm 0.08$ |
| $P_T$(dilepton) | 26 | $-0.54^{+0.35}_{-0.25} \pm 0.16$ | $-0.47 \pm 0.10 \pm 0.09$ |
| $P_T$(lep+jets) | 57 | $0.95^{+0.35}_{-0.42} \pm 0.17$ | $0.11^{+0.21}_{-0.19} \pm 0.10$ |
| $P_T$(combined) | 83 | $0.31^{+0.37}_{-0.23} \pm 0.17$ | $-0.18^{+0.14}_{-0.12} \pm 0.12$ |
| Combined | $\cdots$ | $0.74^{+0.22}_{-0.34}$ | $0.00^{+0.20}_{-0.19}$ |
| 95% C.L. limit | $\cdots$ | $^{<0.95}_{>0.18}$ | $< 0.27$ |

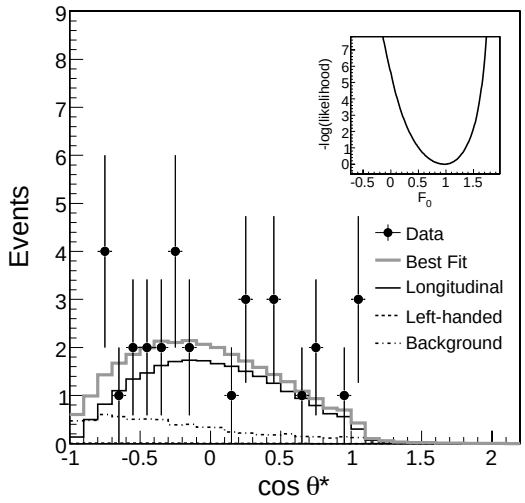


FIG. 2: The $\cos\theta^*$ distribution for the lepton plus jets sample, overlaid with signal and background templates superimposed according to their best-fit values. The inset shows the projection of negative log-likelihood along the $F_0$ axis for the fit to the data.

The data are fit separately to the $\cos\theta^*$ and $P_T$ templates using likelihood functions that include a Gaussian constraint on the background, as well as corrections for trigger and event selection cuts that have helicity-dependent biases, such as those on the lepton $P_T$. We constrain $F_+$ to zero when fitting for $F_0$; when fitting for $F_+$ we constrain $F_0$ to 0.70. The results of the fits to the various subsamples are shown in Table I. The reconstructed $\cos\theta^*$ distribution from the data and the best-fit templates are shown in Figure 2. The observed $\cos\theta^*$ distribution extends somewhat beyond the physical range $-1 \leq \cos\theta^* \leq 1$ because the world-average top and $W$ masses are used in Equation 2, rather than the event-by-event reconstructed masses which have much larger uncertainties. In the dilepton sample, the best-fit value of $F_0$ falls at $-0.54^{+0.35}_{-0.25}$, outside the physical range. In this case, the observed distribution of lepton $P_T$ is softer than any component of signal or background in our model. However, this result is within $2\sigma$ of the lepton plus jets result. Given this level of agreement, we proceed to perform a combined $P_T$ fit to the two samples. The lepton $P_T$ distribution for the two samples and the results of the fit are shown in Figure 3.

The dominant systematic uncertainties in the $\cos\theta^*$ and $P_T$ analyses arise from uncertainties in

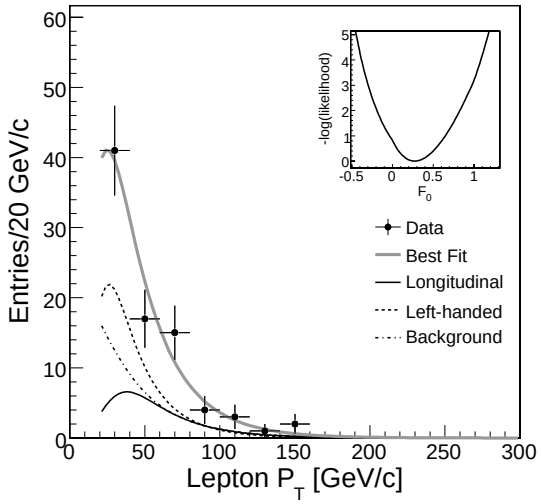


FIG. 3: Distribution of lepton $P_T$ for the lepton plus jets and dilepton samples, overlaid with the total signal and background templates according to their best-fit values. The inset shows the projection of negative log-likelihood along the $F_0$ axis for the fit to the two samples.

the top-quark mass, the background shape and normalization, the effects of initial- and final-state radiation (ISR/FSR), and uncertainty in the parton distribution functions (PDFs). We determine these uncertainties by casting pseudo-experiments in which the systematic parameter in question is varied by $\pm 1\sigma$ and the resulting pseudo-data are fit to the default templates. We compare the mean $F_0$ or $F_+$ returned by the likelihood fit with the default (unfluctuated) value. The results are summarized in Table II. The sum in quadrature of all sources of systematic uncertainty leads to a final result of $F_0 = 0.99^{+0.29}_{-0.35}(\text{stat.}) \pm 0.19(\text{syst.})$ for the $\cos\theta^*$ analysis and $F_0 = 0.31^{+0.37}_{-0.23}(\text{stat.}) \pm 0.17(\text{syst.})$ for the $P_T$ analysis.

TABLE II: Summary of systematic uncertainties for the measurements of $F_0$ and $F_+$.

| Systematic Source | $P_T$ Method | | $\cos\theta^*$ Method | |
|---|---|---|---|---|
| | $\Delta F_0$ | $\Delta F_+$ | $\Delta F_0$ | $\Delta F_+$ |
| Top Mass | 0.11 | 0.09 | 0.08 | 0.04 |
| Bkg. Modeling | 0.10 | 0.06 | 0.13 | 0.05 |
| ISR/FSR | 0.04 | 0.03 | 0.03 | 0.02 |
| PDF | 0.03 | 0.03 | 0.04 | 0.01 |
| MC Statistics | 0.01 | <0.01 | 0.01 | 0.01 |
| Acceptance Correction | 0.02 | 0.01 | $< 0.005$ | $< 0.005$ |
| Trigger Correction | 0.02 | 0.02 | ... | ... |
| Jet Energy Scale | ... | ... | 0.09 | 0.04 |
| MC Modeling | ... | ... | 0.04 | 0.02 |
| $b$-tagging | ... | ... | 0.01 | $< 0.005$ |
| Total | 0.17 | 0.12 | 0.19 | 0.08 |

We combine the results of the $\cos\theta^*$ and $P_T$ analyses taking into account both the statistical and systematic correlations between the two techniques. Statistical correlations arise because the two analyses share the subset of the lepton plus jets sample that passes the $\chi^2_{min}$ cut on the top mass

reconstruction, while common sources of systematic uncertainty include the top mass uncertainty and background normalizations. The correlation coefficients are determined via pseudo-experiments. The combined result is $F_0 = 0.74^{+0.22}_{-0.34}$ (stat.+syst.). In addition, we find $F_+ = 0.00^{+0.20}_{-0.19}$ (stat.+syst.) and $F_+ < 0.27$ at the 95% C.L. These results are consistent with the SM predictions of $F_0 = 0.70$, $F_+ = 0$.

We thank Tim Stelzer and Fabio Maltoni for their help with the MadEvent calculations. We thank the Fermilab staff and the technical staffs of the participating institutions for their vital contributions. This work was supported by the U.S. Department of Energy and National Science Foundation; the Italian Istituto Nazionale di Fisica Nucleare; the Ministry of Education, Culture, Sports, Science and Technology of Japan; the Natural Sciences and Engineering Research Council of Canada; the National Science Council of the Republic of China; the Swiss National Science Foundation; the A.P. Sloan Foundation; the Bundesministerium für Bildung und Forschung, Germany; the Korean Science and Engineering Foundation and the Korean Research Foundation; the Particle Physics and Astronomy Research Council and the Royal Society, UK; the Russian Foundation for Basic Research; the Comision Interministerial de Ciencia y Tecnologia, Spain; in part by the European Community's Human Potential Programme under contract HPRN-CT-2002-00292; and the Academy of Finland.

---

[1] CDF Collaboration, T. Affolder *et al.*, Phys. Rev. D **63**, 0302003 (2001).
[2] DØ Collaboration, V. Abazov *et al.*, Nature **429**, 638 (2004).
[3] M. Cacciari *et al.*, JHEP 0404, 068 (2004).
[4] N. Kidonakis and R. Vogt, Phys. Rev. D **68**, 114014 (2003).
[5] Charge-conjugation symmetry implies that the $\bar{t}$ quark decays to either a longitudinally- or right-handed-polarized $W^-$. Throughout the remainder of this Letter, a "left-handed $W$" refers to either a left-handed $W^+$ or a right-handed $W^-$.
[6] G. L. Kane, G. A. Ladinsky, and C.-P. Yuan, Phys. Rev. D **45**, 124 (1992).
[7] H.S. Do, S. Groote, J.G. Körner, and M.C. Mauser, Phys. Rev. D **67** 091501 (2003); J. Cao et al., Phys. Rev. **D68**, 054019 (2003); E. Malkawi, C.-P. Yuan, Phys. Rev. **D50**, R4462 (1994).
[8] CDF Collaboration, T. Affolder *et al.*, Phys. Rev. Lett. **84**, 216 (2000).
[9] CDF Collaboration, D. Acosta *et al.*, Phys. Rev. D **71**, 031101(R) (2005).
[10] DØ Collaboration, V. M. Abazov *et al.*, Phys. Lett. **B617**, 1 (2005).
[11] CDF Collaboration, D. Acosta *et al.*, Phys. Rev. D **71**, 032001 (2005).
[12] In the CDF geometry, $\theta$ is the polar angle with respect to the proton beam axis, and $\phi$ is the azimuthal angle. The pseudo-rapidity is $\eta \equiv -\ln(\tan(\theta/2))$. The transverse momentum $P_T$ is the component of the momentum projected onto the plane perpendicular to the beam axis. The transverse energy $E_T$ of a shower or calorimeter tower is $E \sin\theta$, where $E$ is the energy deposited.
[13] CDF Collaboration, D. Acosta *et al.*, Phys. Rev. Lett. **93**, 142001 (2004).
[14] CDF Collaboration, D. Acosta *et al.*, Phys. Rev. D **71**, 052003 (2005).
[15] N. Goldschmidt, Ph.D. thesis, University of Michigan (2005).
[16] T. Vickey, Ph.D. thesis, University of Illinois (2004).
[17] F. Maltoni and T. Stelzer, JHEP **02**, 27 (2003).
[18] G. Corcella *et al.*, JHEP **01**, 10 (2001).
[19] T. Sjostrand *et al.*, Comp. Phys. Commun. **135**, 238 (2001).